FR8403369

institut de physique nucléaire

LABORATOIRE ASSOCIÉ A L'IN2P3

IPNO DRE 83-11

DECAYS OF $^{108m+g}$In AND $^{106m+g}$In

B. ROUSSIERE, P. KILCHER, J. SAUVAGE-LETESSIER, C. BOURGEOIS
and the ISOCELE collaboration,

R. BERAUD, R. DUFFAIT, M. MEYER,

J. GENEVEY-RIVIER, J. TREHERNE.

UNIVERSITÉ PARIS SUD

IPNO DRE 83-11

DECAYS OF $^{108m+g}In$ AND $^{106m+g}In$

B. ROUSSIERE, P. KILCHER, J. SAUVAGE-LETESSIER, C. BOURGEOIS
and the ISOCELE collaboration,

R. BERAUD, R. DUFFAIT, M. MEYER,

J. GENEVEY-RIVIER, J. TREHERNE.

DECAYS OF $^{108m+g}In$ AND $^{106m+g}In$

B. ROUSSIERE, P. KILCHER, J. SAUVAGE-LETESSIER, C. BOURGEOIS and the ISOCELE collaboration

Institut de Physique Nucléaire, 91406 Orsay, France

R. BERAUD, R. DUFFAIT, M. MEYER

Institut de Physique Nucléaire, 69622 Villeurbanne Cedex, France

J. GENEVEY-RIVIER, J. TREHERNE

Institut des Sciences Nucléaires, 38026 Grenoble Cedex, France

ABSTRACT

The ^{108}Cd and ^{106}Cd isotopes have been studied from the β^+/EC decay of $^{108m+g}In$ and $^{106m+g}In$, with the ISOCELE facility. Gamma-ray, conversion electron, γ-γ-t and e^--γ-t coincidence measurements have been performed and level schemes of ^{108}Cd and ^{106}Cd have been built. A 0^+ excited state has been clearly established at 1913.2 keV in ^{108}Cd. The properties of the excited states are discussed in terms of vibrator + particle approach and interacting boson approximation. The present results lead us to assign the spin and parity value $I^\pi = 7^+$ for the isomeric state in ^{108}In and in ^{106}In, this is discussed in the framework of the j-j coupling model.

RADIOACTIVITY $^{108,106}In$ [from Sn(^{3}He, 3pxn)In or Sn(p,2pxn)In, on-line mass-separated] ; measured E_γ, I_γ, E_{ce}, I_{ce}, $\gamma\gamma$-, γe^--coin. $^{108,106}Cd$ deduced levels, J, π, ICC, γ-multipolarity, logft. Hyperpure Ge, Si(Li).

1 - INTRODUCTION

Cadmium nuclei belong to the transitional region situated between the semi-magic tin nuclei and those more deformed zirconium. Cadmium ($Z = 48$) and mercury ($Z = 80$) could be expected to have similar properties because they have two protons less than the magic numbers $Z = 50$ and $Z = 82$ respectively. Moreover, the deformation energy curves found for Hg and Cd isotopes show some similarities /1,2/. Except for the semi-magic ^{98}Cd, calculated to be spherical and stiff, the Hg and Cd nuclei are found to be quite soft and their potential energy surfaces have two minima located at around the same energy, one oblate and the other prolate. So the ground states of the even-even Cd nuclei are predicted to be prolate /2/ in good agreement with the experimental Q_{2+} values /3/. Shape coexistence having been clearly established in Hg nuclei /4,5/, we searched for a low-energy 0_2^+ excited state corresponding to an oblate shape in both ^{108}Cd and ^{106}Cd nuclei. These nuclei have already been studied using β^+ decay /6-9/, (^{3}He,d) reactions /10/, (^{3}He,n) reactions /11/, and in-beam experiments /12-14/. Numerous results have been obtained which are not in total agreement, in particular several 0+ excited states have been suggested /10,11,15/ in ^{108}Cd and ^{106}Cd but as yet none of them have been established firmly. In the same way, the spin and parity assignment to $^{108m+g}$In and $^{106m+g}$In is still a much debated question /6,7,8,9,16,17/. Although we could clearly establish a 0+ excited state in ^{108}Cd, there is no evidence of shape coexistence in ^{108,106}Cd. The results presented in this paper clarify the decays of both ground state and isomeric state of ^{106}In and ^{108}In, furthermore they suggest spin and parity values I^{π}=7+ for the isomeric states.

2 - EXPERIMENTAL PROCEDURE

The ^{108}Cd and ^{106}Cd were studied from the β^+/EC decay of the ^{108}In and ^{106}In nuclei. The In isotopes were produced by the Sn(^{3}He(270 MeV), 3pxn)In, Sn(α(200 MeV), 3pxn)In, or Sn(p(200 MeV),2pxn)In reactions. A molten tin target of 1 cm^3 volume placed in the ion source of the ISOCELE II isotope separator was bombarded by ^{3}He, α, or p beam with maximum intensity of 1 μA, 1 μA, and 2 μA respectively. Taking into account the yields of In nuclei obtained with the three kinds of beam /18/, we used the ^{3}He and p beams for the ^{108}Cd and ^{106}Cd studies respectively. The In isotopes produced in the target were mass-separated and the activities obtained were carried from the collecting point to the counting station by means of a mechanical tape transport system. The ^{108,106}Cd isotopes are stable and for these masses, only the In nuclei are extracted from the target, consequently the detected gamma-rays

correspond to the In $\rightarrow$ Cd decays. Singles gamma-rays were measured using two coaxial Ge(HP) detectors (resolution 1.8 keV FWHM at 1332 keV). In order to calibrate these gamma detectors in energy, we
detected gamma-rays simultaneously emitted by ^{108}In (or ^{106}In) and ^{226}Ra sources. The conversion electron spectra were obtained using a cooled Si(Li) detector with a thickness of 3 mm and an active area of 300 mm^2 (resolution 2.7 keV FWHM at 624 keV). γ-γ-t and e^--γ-t coincidence measurements were performed. The linear signals coming from the detectors and the time difference signal were digitized and recorded in event-by-event mode on magnetic tapes. Further details of this experimental set up can be found in ref. /19/.

Moreover, in order to eliminate the very inconvenient β^+-background observed up to $\sim$2.5 MeV in the ^{106}Cd study /20/, a conversion-electron spectrum was measured using a cooled Si(Li) detector associated to a selecting magnetic field /21/, perfected by Paris.

3 - EXPERIMENTAL RESULTS

3.1 - The ^{108}Cd nucleus

The energy of the first 0^+ excited state in the heavier even-even Cd nuclei increases when the mass decreases : 1134 keV in ^{114}Cd, 1224 keV in ^{112}Cd, and 1473 keV in ^{110}Cd. Consequently an energy range up to 2 MeV was chosen for the electron measurements. Figure 1 shows singles gamma-ray and conversion-electon spectra. All the results are listed in table 1. From the pure E2 transition of 632.9 keV ($2_1^+ \rightarrow 0_1^+$) taken as reference, the conversion coefficients α_K of the main transitions have been calculated and the most probable multipolarities deduced using the theoretical α_K values of Hager and Seltzer /22/. In this way the conversion coefficient of the 1913.2 keV transition has been found to be very large : α_K (1913.2 keV) > 10 $\alpha_{K\ th.}$(M4), which clearly determines an E0 multipolarity for this transition.

From the γ-γ coincidence results given in table 1, a level scheme of ^{108}Cd has been established (fig.2). It is in good agreement with those reported before by several authors /6,9,10,12/. Thus we shall discuss here the new or confirmed main results :

- A spin and parity value $I^{\pi}=0^+$ is assigned to the level at 1913.2 keV since it decays by an E0 transition to the ground state. It could correspond to the 0^+ level at 1.9 MeV populated in the (^{3}He,n) reaction /11/. This level has also been observed by Flanagan et al. /6/, who suggested $I^{\pi} = 2^+$ for this state.
- The $I^{\pi}=3+$ assignment is suggested for the level at 2162.6 keV due to the E1 character of the 1529.7 keV transition to the 2_1^+ state.
- The new levels lying at 3367.3 keV, 3816.0 keV, 4043.4 keV, 4179.0 keV, 4239.6 keV, 4251.2 keV, 4512.3 keV, and 4525.2 keV have been established from coincidence data but the transitions deexciting these levels are too weak to allow conversion coefficient determination and consequently J^{π} assignments.

3.2 - The ^{106}Cd nucleus

Singles gamma-ray and conversion-electron spectra are shown in figure 3 and all the results listed in table 2. Experimental methods were the same as for the ^{108}Cd study and the 632.7 keV pure E2 transition has been used as reference to determine the conversion coefficients.

The first electron spectra had suggested the existence of a 0^+ state at 2034.8 keV /19,20/ but this result has not been confirmed by the conversion-electron measurements performed more precisely with a Si(Li) detector placed in a magnetic field to eliminate the β^+ background.

The level scheme, shown in figure 4, has been built on the basis of coincidence relationships, energies, and relative intensities of the transitions listed in table 2. It has numerous levels in good agreement with the previous studies /7,8,9,13,14/. In addition five new levels lying at 2600.5 keV, 3284.1 keV, 3472.2 keV, 4243.9 keV and 5131.0 keV have been established. Two other levels can be located at 2034.8 keV and 4398.6 keV but only one transition is deexciting each of them. Finally we have to note that the 3284.1 keV level decays through the 780.7 keV and 792.5 keV transitions which are in coincidence with the 1009.4 keV and 997.9 keV lines respectively. A 780.5 keV gamma-line had already been observed by Danière et al. /13/ and Samuelson et al.

/14/ who placed it between the 3409.6 keV and 2629.3 keV levels. The 780.7 keV gamma-ray that we have observed in the present work being in coincidence with the 1009.4 keV and not with the 524.5 keV and 1135.8 keV lines, we conclude that two different 781 keV transitions exist in ^{106}Cd : a 780.5 keV transition observed in (H I,xnγ) reactions and a 780.7 keV transition observed in β^+/EC decay of the ^{106}In nucleus (Fig. 5).

3.3 - Spin values of the isomeric states of ^{108,106}In.

Spins of the isomeric states of ^{108}In and ^{106}In have already been discussed by several authors /6,7,8,9,16,17/. The relative location of the ground and isomeric state is not known. We shall assume that the high spin state is the isomeric one in ^{108,106}In like in the heavier odd-odd In nuclei. In our studies the relative intensities of the γ-rays were followed for several hours in order to determine the proportion of ^{108g}In and ^{108m}In in the source. So the yield of ^{108}In in its low-spin state has been calculated to be arround 15%. A similar result was found for ^{106g}In and ^{106m}In from the comparison of our results with those reported in ref. 7 . As more than 95% of the total γ-ray intensity has been placed in ^{106,108}In decay schemes, the logft values has been calculated for the most directly populated states (see table 3).

In ^{108}Cd the 5^- level located at 2601.5 keV is populated by five weak γ-rays and is not directly fed by the β^+/EC decay, contrary to previous results /6,9/ . A direct evidence of this fact is shown in figure 6. Indeed, the 1093.2 keV γ-ray deexciting this 2601.5 keV level is not coincident with the 511 keV annihilation line but only with the X-ray lines in contrast with the 1299.3 keV γ-ray deexciting the 6^+ level located at 2807.5 keV. Therefore, this 5^- level in ^{108}Cd is not directly fed by the β^+/EC decay of ^{108}In but is fed through upper levels, the feeding of which mainly proceeds via electron capture. On the other hand, the 3110.1 keV (8^+), 2993.8 keV (6^+), and 2807.5 keV (6^+) levels are fed clearly by the decay of ^{108}In : 60% of the β^+/EC decay proceeds to these three levels and the deduced logft values are only consistent with an allowed transition ($\Delta I = 0,1$ and $\Delta\pi = +$). From all these results we assign the spin and parity value $I^\pi = 7^+$ for the isomeric state of ^{108}In.

In ^{106}Cd three states are mainly populated by the β^+/EC decay of ^{106}In : the 8^+ state located at 3044.4 keV and the 6^+ states at 2503.3 keV and 2491.8 keV. The logft values calculated for these states are given in table 3. They lead us to assign the spin and parity value $I^\pi = 7^+$ for the isomeric state of ^{106}In contrary to the assignment 5^+ or 6^+ suggested in the references /7,9/.

4 - DISCUSSION

In order to interpret the 0^+ excited state observed in the ^{108}Cd nucleus, let us compare the low-lying excited states of the ^{108,106}Cd isotopes to those known in the heavier even-even Cd nuclei (Fig. 7). The 0_2^+ state in $^{110-116}$Cd is always located just below the 2_2^+ and 4_1^+ states whereas the first excited 0^+ level observed in ^{108}Cd is lying far above the 2_2^+ and 4_1^+ states. The Cd isotopes are usually considered as vibrational nuclei with a typical triplet 0_2^+, 2_1^+, 4_1^+ located at around 1.3 MeV excitation energy. This is true between A = 116 and 110 but in ^{108}Cd, the 0^+ state we have observed is too high in energy to belong to such a vibrational triplet. Since no band structure has been observed on it, the 0^+ excited state of ^{108}Cd cannot be interpreted as a collective band-head corresponding to an oblate-shaped nucleus.

The properties of the low-spin states of even-even Cd nuclei have been calculated using a vibrational approach : either with the particule-vibrator coupling model /23,24/ or with the interacting boson model IBM /25/, which are almost equivalent since only the mathematical treatment is different. On the other hand the properties of the high-spin states of Cd nuclei have been calculated in the framework of the two quasiparticles -plus-rotor model (rotor + 2qp) using a weak deformation /12-14/. For the In nuclei, the spin and parity values of the ground-state and isomeric state have been calculated using the rotor+qp model (^{108}In) /27/ and the j-j coupling (^{110}In) /28/. The Cd and In nuclei are situated near the Z = 50 closed shell, they are weakly deformed and belong to a transitional region, so their properties can be explained either with a vibrational description or with a rotational one, as indicated in ref.29 for the odd-A In nuclei /29/ . Thus we can compare the experimental results to the calculations already performed.

Within the particle -vibrator coupling model, Lopac /23, 24/ calculated the low-lying states of ^{108}Cd. The energies and the deexcitation modes of the 2_1^+, 4_1^+ and 2_2^+ levels have been rather well reproduced but in this model the 0_2^+ state is found to decay mainly to the first 2_1^+ level and weakly to the 2_2^+ state contrary to our experimental results (Fig. 8 and Table 4).

Recently the even-even Cd nuclei have been interpreted by Sambataro in the framework of the interacting boson approximation with mixing procedure developed to take into account excitations of two protons accross the shell-gap /25/. These calculations have in particular explained the presence of intruder 0_3^+ and 2_3^+ states observed at an energy similar to that of the two-phonon triplet in $^{110-116}$Cd. Although only one 0^+ excited state was observed in ^{108}Cd, it is interesting to compare the experimental ^{108}Cd level scheme to the IBM results. Indeed, the energies and the deexciting modes of the 2_1^+, 4_1^+ and 2_2^+ levels are well reproduced in $^{106-116}$Cd by such calculations. On the other hand, the calculations of Sambataro on the ^{112,114}Cd nuclei show that the 0_3^+ state decays mainly to the 2_2^+ state like the 0^+ excited state observed in ^{108}Cd, which suggests that this 0^+ state has the same configuration as the 0_3^+ states observed in ^{112,114}Cd, i.e. two-particle two-hole excitation. If this is true, the question of non-observation of a 0^+ state below 1.9 MeV remains.

We can notice that for A = 114 and 112 the 0_2^+ state is more populated than the 0_3^+ state by the β^+/EC decay of the 1^+ ground state of In /26/. Contrarily for A = 110, only 0_3^+ level is populated by the decay of the 2^+ ground state of In. Therefore, if the ^{108g}In and ^{110g}In nuclei have the same spin and parity values, 0^+ excited level observed in ^{108}Cd could be a state similar to the 0_3^+ level of the heavier even-even Cd nuclei.

Recently, in the framework of a slightly deformed rotor+two quasi-particle model, calculations have been performed to interpret results obtained in ^{108}In /27/. So the positive parity states have been found to correspond to (Ω = 9/2, $\pi g_{9/2}$) (Ω = 3/2, $\nu g_{7/2}$) and (Ω = 9/2, $\pi g_{9/2}$) (Ω = 5/2, $\nu d_{5/2}$) configurations which give the (6^+ - 3^+) and (7^+ - 2^+) doublets respectively but the 6^+ state was not located exactly with respect to the 7^+ state. On the other hand the In nuclei are weakly deformed ($\beta \sim 0.1$), which means that the coupling rules established by Nordheim /30/ and then by Brennan and Bernstein /28/ in the framework of a j-j coupling using the spherical subshells can likely be applied to the odd-odd In isotopes. Thus the spin and parity values of the low-lying states of these isotopes can be deduced from the ground state configurations of the neighbouring odd-Z and odd-N nuclei. All the $_{49}$In isotopes have a $9/2^+$ ground state arising from the $(1g_{9/2})^{-1}$ proton configuration. The ground state of the N = 51, 53, and 55 Cd or Pd nuclei have spin and parity value $I^\pi = 5/2^+$ coming from the $2d_{5/2}$ subshell. However the ground state of the N = 57, 59, and 61 Cd and Pd nuclei having also $5/2^+$ as spin and parity value it seems that the pairing energy is large enough in the $1g_{7/2}$ neutron subshell so that the neutrons are filling the $1g_{7/2}$ subshell before the $2d_{5/2}$ is filled up. Therefore the most probable configurations for the low-lying states in ^{108}In (^{106}In) are $\pi g_{9/2}^{-1}$ $\nu d_{5/2}^{-1}$ or $\pi g_{9/2}^{-1}$ $\nu d_{5/2}^{-3}$ with 2 or 3 (1 or 2) neutron pairs in the $g_{7/2}$ shell. We have to remark that these two configurations are obtained by removing one (for ^{108}In) or two (for ^{106}In) neutron pairs from the configuration suggested for ^{110}In in reference /28/. For these π hole-ν hole configurations, the rules of Brennan and Bernstein lead to $I^\pi = 7^+$ and 2^+ for the lowest-lying states. Another configuration for ^{106}In could be $\pi g_{9/2}^{-1}$ $\nu d_{5/2}$, as it is suggested in reference /7/, but the j-j coupling rules would then lead to $I^\pi = 6^+$ which is inconsistent with our experimental results (cf. 3.3).

5 - CONCLUSION

We have built level schemes of $^{108,106}Cd$ from the β^+/EC decay of $^{108,106}In$. An excited 0^+ state has been clearly established in the ^{108}Cd nucleus. This 0^+ state can be understood neither in terms of shape coexistence, nor as member of vibrational triplet. Its decay properties are very similar to those of the 0_3^+ states in the heavier even-even Cd nuclei. Because of the absence of another 0^+ at lower energy, it is not possible to extend to ^{108}Cd the IBM calculation used for $^{112,114}Cd$ nuclei. But it would be fruitful to extend to low-spin states the axial rotor + 2qp calculations that Samuelson et al. used to interpret high spin states of $^{108,106}Cd$ observed in H.I. reactions /12,14/.

The present experimental investigations indicate a spin and parity value $I^\pi = 7^+$ for the $^{108,106}In$ high spin isomeric state (or ground state). This spin and parity value can be explained in the framework of the j-j coupling as $\pi g_{9/2}^{-1}\ \nu d_{5/2}^{-1}$ or $\pi g_{9/2}^{-1}\ \nu d_{5/2}^{-3}$ configuration. These configurations leading to $I^\pi = 7^+$ and 2^+, we suggest the spin and parity value $I^\pi = 2^+$ for the ground state (or isomeric state) of $^{108,106}In$.

ACKNOWLEDGEMENTS

We would like to thank the staff of the Isocele separator for technical assistance especially J. Obert and J.C. Putaux for the target-ion-source system developments. We are indebted to the staff of the Orsay synchrocyclotron for their cooperation. We thank Dr. P. Paris who allowed us to use the "Si(Li) electron detector + magnetic selector" system and Dr. M.I. Marques who participated in the experiments.

REFERENCES

/1/ M. CAILLIAU, J. LETESSIER, H. FLOCARD and P. QUENTIN
Phys. Lett. 46B (1973) 11

/2/ M. MEYER, J. DANIERE, J. LETESSIER and P. QUENTIN,
Nucl. Phys. A316 (1979) 93

/3/ M.T. ESAT, D.C. KEAN, R.H. SPEAR and A.M. BAXTER,
Nucl. Phys. A 274 (1976) 237

/4/ R. BERAUD, M. MEYER, M.G. DESTHUILLIERS, C. BOURGEOIS, P. KILCHER and J. LETESSIER, Nucl. Phys. A284 (1977) 221

J. BONN, G. HUBER, H.J. KLUGE, V. KOPF, L. KUGLER and E.W. OTTEN,
Phys. Lett. 36B (1971) 41

/5/ J.H. HAMILTON, Proceedings on the International Conference on Selected Topics in Nuclear Structure, edited by V.G. Soloviev et al. (Dubna , USSR, 1976), vol. II, p. 303

/6/ S. FLANAGAN, R. CHAPMAN, G.D. DRACOULIS, J.L. DURELL, W. GELLETLY, A.J. HARTLEY and J.N. MO, J. Phys. G1 (1975) 77

/7/ S. FLANAGAN, R. CHAPMAN, J.L. DURELL, W. GELLETTY and J.N. MO, J. Phys. G2 (1976) 589

/8/ H. HUANG, B.P. PATHAK, J.K. LEE, Can. J. Phys. 56 (1978) 936

/9/ I.N. WISCHNEWSKI, H.V. KLAPDOR, P. HERGES, H. FROMM and W.A. ZHELDONOZHSKI, Z. Phys. A298 (1981) 21

/10/ R.L. AUBLE, D.J. HOREN, F.E. BERTRAND and J.B. BALL, Phys. Rev. 6 (1972) 2223

/11/ H.W. FIELDING, R.E. ANDERSON, C.D. ZAFIRATOS, D.A. LIND, F.E. CECIL and H.H. WIEMAN, Nucl. Phys. A281 (1977) 389

/12/ L.E. SAMUELSON, F.A. RICKEY, J.A. GRAU, S.I. POPIK and P.C. SIMMS, Nucl. Phys. A301 (1978) 159

/13/ J. DANIERE, R. BERAUD, M. MEYER, R. ROUGNY, J. GENEVEY-RIVIER and J. TREHERNE, Z. Physik A280 (1977) 363

/14/ L.E. SAMUELSON, J.A. GRAU, S.I. POPIK, F.A. RICKEY and P.C. SIMMS, Phys. Rev. C19 (1979) 73

/15/ K. CORNELIS, E. COENEN, M. HUYSE, G. LHERSONNEAU and J. VERPLANCKE, 4th Int. Conf. on nuclei far from stability, Helsingor (1981) CERN 81-08 p. 460

/16/ D.C. STROMSWOLD, D.O. ELLIOT, Y.K. LEE, L.E. SAMUELSON, J.A. FRAU, F.A. RICKEY and P.C. SIMMS, Phys. Rev. C17 (1974) 143

/17/ L. VANNESTE, D. VANDEPLASSCHE, E. VAN WALLE, J. GEENEN, C. NUYTTEN, and H. MARSHAK, 4th Int. Conf. on nuclei far from stability, Helsingor (1981) CERN 81-08 p. 26
L. VANNESTE, D. VANDEPLASSCHE, E. VAN WALLE, C. NUYTTEN, Proceedings of the International Conference on Nuclear Structure (1982) Amsterdam p. 262

/18/ J.C. PUTAUX, J. OBERT, L. KOTFILA, B. ROUSSIERE, J. SAUVAGE-LETESSIER, C.F. LIANG, A. PEGHAIRE, P. PARIS and J. GIROUX, Nucl. Instr. Meth. 186 (1981) 321

/19/ B. ROUSSIERE, Thèse 3ème cycle (1981) Paris

/20/ B. ROUSSIERE , P. KILCHER, J. SAUVAGE-LETESSIER, R. BERAUD, R. DUFFAIT, M. MEYER, J. GENEVEY-RIVIER, and J. TREHERNE, 4th Int. Conf. on nuclei far from stability, Helsingor (1981) CERN 81-08 p. 465

/21/ P. PARIS and J. TREHERNE, Rev. Phys. Appl. 4 (1969) 291

/22/ S. HAGER and E.C. SELTZER, Nucl. Data A4 (1968) 2

/23/ G. ALAGA, F. KRMPOTIC and V. LOPAC, Phys. Lett. 24B (1967) 537

/24/ V. LOPAC, Ph. D. Thesis (1971) Zagreb

/25/ M. SAMBATARO, Nucl. Phys. A380 (1982) 365

/26/ C.M. LEDERER and V.S. SHIRLEY, Table of Isotopes, 7th edition (1978)

/27/ N. ELIAS, R. BERAUD, A. CHARVET, R. DUFFAIT, M. MEYER, S. ANDRE, J. GENEVEY, S. TEDESCO, J. TREHERNE, F. BECK and T. BYRSKI, Nucl. Phys. A351 (1981) 142

/28/ M.H. BRENNAN and A.M. BERNSTEIN, Phys. Rev. 120 (1960) 927

/29/ K. HEYDE, M. WAROQUIER, P. VAN ISACKER and H. VINCX, Nucl. Phys. A292 (1977) 237

/30/ L.W. NORDHEIM, Phys. Rev. 78 (1950) 294

/31/ N.B. GOVE and M.J. MARTIN, Nucl. Data Tables 10 (1971) 206

TABLE CAPTIONS

TABLE 1 : Gamma-ray and internal-conversion electron data for the decay of $^{108m+g}In$ to ^{108}Cd (energy error $\sim$0.2 keV and intensity error $\sim$10%)

TABLE 2 : Gamma-ray and internal-conversion electron data for the decay of $^{106m+g}In$ to ^{106}Cd (energy error $\sim$0.2 keV and intensity error $\sim$10%)

TABLE 3 : Logft values for the most populated states of $^{108,106}Cd$ nuclei by the β^+/EC decay of the high spin state of $^{108,106}In$. The proportion of $^{108,106}In$ in its high spin state in the sources was calculated to be around 85%. The Q_{EC} and $T_{1/2}$ value are taken from ref.20 and the $\log f_o$ values from the ref.31

TABLE 4 : Experimental and theoretical values of transition probabilities (in e^2b^2) and branching ratios in ^{108}Cd. The theoretical values are taken from ref. 24.

FIGURE CAPTIONS

FIGURE 1 : Singles γ-ray spectrum (A) and internal conversion electron spectrum (B) from sources of $^{108m+g}$In.

FIGURE 2 : Level scheme of ^{108}Cd. For sake of clearness the quasi rotational bands are shown on the left of the figure.

FIGURE 3 : Single γ-ray spectrum (A) and internal conversion electron spectrum (B) from sources of $^{106m+g}$In.

FIGURE 4 : Level scheme of ^{106}Cd. For sake of clearness the quasirotational bands are shown on the left of the figure.

FIGURE 5 : Coincidence spectrum for ^{106}In decay corresponding to a gate set on the 780.7 keV γ-ray line. B.S. refers to coincident back-scattered peak.

FIGURE 6 : Coincidence spectra for ^{108}In decay corresponding to gates set on 1299.3 keV and 1093.2 keV γ-ray lines.

FIGURE 7 : Systematics of first excited levels in Cadmium isotopes.

FIGURE 8 : Experimental and theoretical first excited levels scheme of ^{108}Cd. The theoretical levels have been calculated using an harmonic vibrator coupled with two proton holes /24/

Table 1

E_γ	I_γ	$I_{e^-} \times 10^3$	Multipolarity	Main coincident transitions	Location
166.1	0.18			875, 1057, (1530)	
206.1	0.36			633, 875, 1093	2807.5 - 2601.5
242.6	30	1000	M1	326, 633, 637, 731, 875, 969, 1008, 1057, 1432, 1443, 1606	2807.5 - 2564.9
266.4	2.3			633, 875, 1033	2807.5 - 2541.1
311.5	0.2			969	1913.2 - 1601.7
325.6	10	180	M1	243, 633, 637, 731, 875, 969, 996, 1251, 1606, 1614, 1675, 1729, 1947, 1960	2564.8 - 2239.1
350.4	0.29			633, 875, 1199	3057.4 - 2706.9
373.7	0.42			633, 875, 1093	2975.2 - 2601.5
403.3	0.19			633, 875, 1033	
414.1	0.21				
419.1	0.17				
448.7	0.33			826	3816.0 - 3367.3
455.9	0.31			(243), 875, 1093	3057.4 - 2601.5
494.6	0.17			875, 1033	
542.1	0.15				
544.1	0.12				
555.8	0.36				
569.0	4.2	16	E2	633, 875, 1033	3110.1 - 2541.1
632.9	100	300	E2	243, 266, 326, 350, 374, 456, 569, 637, 648, 708, 731, 755, (760), 770, 875, 969, 1033, 1057, 1088, 1093, 1137, 1142, 1199, 1230, 1247, 1280, 1282, 1299, 1322, 1486, (1513), 1530, 1606, 1733, 1987, 2049, 2223, 2307	632.9 - 0
637.4	1.3			243, 326, 969	2239.1 - 1601.7
648.3	2.6			633, 875, 1033	3189.4 - 2541.1
666.5	0.26				
672.4	0.43				

Table 1 (continued)

708.0	0.46			633, 648, 875, 1033	3897.4 - 3189.4
730.8	6.8	15.6	72%E2+28%M1	243, 326, 633, 755, 875	2239.1 - 1508.3
754.7	1.3			633, 637, 731, 875	2994.0 - 2239.1
760.0	0.40			633, 1513	4512.3 - 3751.9
768.3	0.10				
770.5	0.46			1282	3561.1 - 2790.7
780.7	0.13				
826.2	0.74			449, 633, 875, 1033	3367.3 - 2541.1
871.4	1.1				
875.4	73	105	E2	243, 266, 326, 350, 374, 569, 633, 648, 731, 755, 826, 1033, 1057, 1093,1137, 1142, 1199, 1230, 1247, 1282,1299, 1322, 1486, 1490, 1638, 1692,1805, 1927, 1940, 2223, 2307	1508.3 - 632.9
964.9	0.09				
968.8	2.0	2.8	M1	243, 326, 633, 637	1601.7 - 632.9
996.1	0.54			326, 633, 1057	3561.1 - 2564.9
1008.5	0.45			243, 326, 633, 731, 875, 1057, 1299	3816.0 - 2807.5
1020.1	0.21				
1032.8	17	16	E2	266, 569, 633, 648, 826, 875, 1142,1275, 1409, 1503, 1795, 1984	2541.1 - 1508.3
1050.2	0.25				
1056.6	21	22	M1	243, 633, 875, 996, 1251, 1614, 1675, 1729, 1947	2564.8 - 1508.3
1063.5	0.44				
1087.6	0.40			633	1720.5 - 632.9
1093.2	4.0	1.2	E1	206, 374, 456, 633, 875, 1692, 1923	2601.5 - 1508.3
1137.2	0.82			633, 875	2645.5 - 1508.3
1142.0	1.1	0.81	E2	633, 875, 1033	3683.1 - 2541.1
1167.2	0.29				

Table 1 (continued)

1189.3	0.26				
1198.6	2.3	0.51	E1	350, 633, 875	2706.9 - 1508.3
1214.7	0.13				
1222.0	0.15				
1230.3	0.59			633, 875	2738.6 - 1508.3
1240.6	0.89			633, 875, 1033	3787.7 - 2541.1
1251.4	0.35			1057	3816.0 - 2564.8
1255.1	0.11				
1257.3	0.50			633, 875, 1486	4251.2 - 2994.0
1275.1	0.54			633, 875, 1033	3816.0 - 2541.1
1280.3	0.22			633	1913.2 - 632.9
1282.4	0.71			633, 770, 875	2790.7 - 1508.3
1299.3	11.0	5.7	E2	633, 875	2807.5 - 1508.3
1304.7	0.40				
1322.0	1.4			633, 731, 875	3561.1 - 2239.1
1363.6	0.10				
1367.4	0.31				
1371.9	0.11				
1375.1	0.09				
1387.8	0.49			633	2020.7 - 632.9
1397.5	0.93			633, 875, 1137	4043.4 - 2645.5
1408.8	0.41			633, 875, 1033	3949.9 - 2541.1
1417.9	0.11				
1432.0	0.50			243, 326, 633, 875, 1057, 1299	4239.6 - 2807.5
1443.5	0.41			243, 326, 633, 875	4251.2 - 2807.5
1467.7	0.35			875, 1093	
1485.8	3.2	1.4	E2	633, 875, 1257	2994.0 - 1508.3
1489.7	0.34			875, 1033	
1502.7	0.64			633, 875, 1033	4043.4 - 2541.1

Table 1 (continued)

1512.8	1.0			633, 731, 760, 875	3751.9 - 2239.1
1529.7	2.1	0.39	E1	633	2162.6 - 632.9
1534.2	0.25				
1569.2	0.60			633, 875	
1601.8	2.2	0.81	E2	637	1601.7 - 0
1606.3	6.2	1.9	E2	243, 326, 633, 755, 1322	2239.1 - 632.9
1614.2	0.39			(326), 633, 875, 1057	4179.0 - 2564.9
1622.7	0.22			633, 875	
1638.1	0.77			633, 875, 1033	4179.0 - 2541.1
1661.2	0.11			969	
1665.5	0.22				
1674.9	0.23			326, 633, 875, 1057	4239.6 - 2564.8
1681.1	0.12				
1691.9	0.35			633, 875, 1093	4293.4 - 2601.5
1729.1	0.29			326, 633, (731), 875, 1057	
1732.8	0.97	0.33	E2	633	2365.7 - 632.9
1741.8	0.29			(326), 633	
1784.0	0.29				
1794.8	0.22			569, 875, 1033	4904.9 - 3110.1
1805.2	0.56			633, 875, 1199	4512.3 - 2706.9
1848.3	0.13				
1852.8	0.77			633, 875	
1858.9	0.41			449, 875	3367.3 - 1508.3
1866.6	0.12				
1904.1	0.12				
1911.4	0.13			633, 875, 1093	4512.3 - 2601.5
1913.2	<0.1	1.2	E0		1913.2 - 0
1923.5	0.39			633, 875, 1093	4525.2 - 2601.5
1927.3	0.42			633, 875	

Table 1 (continued)

1939.8	0.18			633, 731	4179.0 - 2239.1
1947.4	0.43			326, 633, 731, 1057	4512.3 - 2564.8
1959.9	0.22			326, (1033), 1057	
1970.9	0.12				
1984.3	0.51			633, 875, 1033	4525.2 - 2541.1
1986.9	3.3	1	E2	633	2619.8 - 632.9
2049.4	0.79			633	2682.3 - 632.9
2222.9	0.53			633, 875	3731.2 - 1508.3
2225.5	0.36				
2307.5	0.58			633, 875	3816.0 - 1508.3
2414.8	0.30				
2440.8	0.22				
2671.5	0.50				

Table 2

E_γ	I_γ	$I_{e^-} \times 10^3$	Multipolarity	Main coincident transitions	Location
161.1	0.23			226, 611, 837	2491.8 - 2330.5
225.9	5.1	260	70%M1+30%E2	161, 388, 553, 593, 611, 633, 754, 861, 875, 1143, 1472	2330.5 - 2104.5
282.7	0.16			593, 754	3367.1 - 3084.5
308.9	0.1				
314.6	0.25				
387.7	0.57	8.7	E2	226, 1084	2104.5 - 1716.6
390.7	0.27				
395.5	0.21				
421.3	0.16	2.4	E2	(593), (623), (1472)	3547.7 - 3126.6
433.0	2.7	25	E2	633, 861, 998	2924.8 - 2491.8
438.6	0.23				
495.6	0.15			611, 861, (1472)	2600.5 - 2104.5
524.3	1.2	2.1	E1	611, 1472	2629.3 - 2104.5
541.0	10	54	E2	633, 861, 1009	3044.4 - 2503.3
552.6	19	84	E2	633, 861, 998	3044.4 - 2491.8
581.2	0.6	2.8	M1	1009	3084.5 - 2503.3
592.9	2.3	9.6	M1	226, (283), 633, 861, 998	3084.5 - 2491.8
601.4	0.44	1.9	M1	887, 1139	4243.9 - 3642.3
610.8	6	21	E2	226, 524, 633, 754, 861	2104.5 - 1493.9
623.3	1	3.9	94%M1+6%E2	1009	3126.6 - 2503.3
632.7	100	300	E2	226, 433, 524, 541, 553, 581, 593, 601, 611, 623, 754, 781, 792, 808, 811, 820, 837, 861, 875, 887, 981, 998, 1009, 1027, 1032, 1064, 1084, 1136, 1139, 1143, 1163, 1217, 1426, 1431, 1472, 1489, 1620, 1715, 1853, 1934	632.7 - 0
636.2	2.4				

Table 2 (continued)

(2)

690.9	0.29				
753.8	1.5	2.6	E2	226, 611, 633, 837, 861, 1472	3084.5 - 2330.5
780.7	1.1	1.8	E2	633, 861, 1009	3284.1 - 2503.3
792.5	0.43			633, 861, 998	3284.1 - 2491.8
802.1	0.48				
808.3	0.53			1009	
811.3	1.7	3	M1	633, 861	2305.2 - 1493.9
820.3	0.49			611, 1472	2924.8 - 2104.5
836.8	2.1			161, 553, 633, 754, 861, 1143	2330.5 - 1493.9
861.2	83	120	E2	226, 433, 524, 541, 553, 593, 611, (623), 633, 754, (781), 793, 811, 837, 875, 981, 998, 1009, 1139, 1149, 1426, 1431	1493.9 - 632.7
875.2	1.4	2.1	E2	633, 861, 998, 1032, 1763	3367.1 - 2491.8
887.1	0.47			601, 633, 861, 1009, 1139	5131.0 - 4243.9
980.8	0.33			861, 998	3472.9 - 2491.8
997.9	39	36	E2	433, 553, 593, 633, 793, 861, 875	2491.8 - 1493.9
1009.4	24	23	E2	541, 623, 633, 781, 861, 1139	2503.3 - 1493.9
1027.5	0.42			226, 611	3357.9 - 2330.5
1031.6	0.8			875, 998	4398.6 - 3367.1
1063.7	0.44				
1076.9	0.25				
1083.9	0.88	1	M1	633	1716.6 - 632.7
1135.8	0.68			861	2629.3 - 1493.9
1138.8	1.8	1.5	M1	601, 633, 861, 1009, 1489	3642.3 - 2503.3
1142.7	1.6			226, 611, 837, 1472	3472.9 - 2330.5
1149.4	0.68			633, 861, 998, 1489	3642.3 - 2491.8
1162.7	0.32			633	1795.4 - 632.7
1173.7	0.26				

Table 2 (continued)

1199.7	0.24			541, 553, 998	4243.9 - 3044.4
1217.5	0.64			226, 611, 837, 861	3547.7 - 2330.5
1243.3	0.13				
1284.6	0.26			633, 861, 1009	3787.6 - 2503.3
1295.4	0.23			998	3787.6 - 2491.8
1298.8	0.29				
1373.6	0.25				
1402.1	0.33			(633)	2034.8 - 632.7
1426.5	0.65			633, 861	2920.4 - 1493.9
1431.0	1.2			633, 861	2924.8 - 1493.9
1442.7	0.38			611, (633), 1472	3547.7 - 2104.5
1471.9	4.3	2	E2	226, 524, 633, (1371),(1443)	2104.5 - 632.7
1488.7	0.96			633, 861, 1009, 1139, 1149	5131.0 - 3642.3
1505.9	0.15			633, 861	
1518.6	0.13				
1524.9	0.59				
1550.5	0.41				
1620.2	0.88			633	2252.9 - 632.7
1622.1	0.49				
1633.2	0.19				
1714.9	2.8			633	2347.6 - 632.7
1716.7	1.3			388	1716.6 - 0
1757.1	0.2				
1763.4	0.53			633, 861, 875, 998	5131.0 - 3367.1
1853.3	0.80			(226), 309, 611, 633, 861	
1896.4	0.39				
1933.6	1.4			633	2566.3 - 632.7
1978.9	0.36			861	3472.9 - 1493.9
2005.3	0.12			633, 861	
2046.2	0.34			611	
2087.1	0.48			(553), 633, (861)	5131.0 - 3044.4

Table 2 (continued)

2148.9	0.15			633, 861	3642.3 - 1493.9
2225.7	0.47			633, 861	
2256.9	0.9			633	
2284.5	0.24			633	2917.6 - 632.7
2390.3	0.21			1009	
2414.1	0.21			611	
2449.0	0.24			226, 611, 633, 861	
2486.5	0.18			633	3119.3 - 632.7
2494.3	0.17			524, 861	
2551.4	0.23			633, 998	
2586.2	0.21			(633), (861)	
2600.7	0.11				2600.5 - 0
2861.6	0.17			633	3494.5 - 632.7
2917.6	0.75				2917.6 - 0
3119.3	0.18				3119.3 - 0
3494.5	0.49				3494.5 - 0

Table 3

	^{108}Cd			^{106}Cd		
E(keV)	2807.5	2993.8	3110.1	2491.8	2503.3	3044.4
I^{π}	6+	6+	8+	6+	6+	8+
Feeding	50%	5%	5%	35%	12%	12%
logft	5.1±0.2	5.9±0.2	5.9±0.2	5.4±0.2	5.9±0.2	5.6±0.2

Table 4

Transition	$B(E2)_{exp.}$	$B(E2)_{th.}$
$2_1^+ \rightarrow 0_1^+$	0.082	0.008
$2_2^+ \rightarrow 0_1^+$	0.0059	0.003
$4_1^+ \rightarrow 2_1^+$	0.122	0.130

Branching ratio	Experiment	Theor
$\frac{0_2^+ \rightarrow 2_2^+}{0_2^+ \rightarrow 2_1^+}$	1070	0.05
$\frac{2_2^+ \rightarrow 2_1^+}{2_2^+ \rightarrow 0_1^+}$	11	23

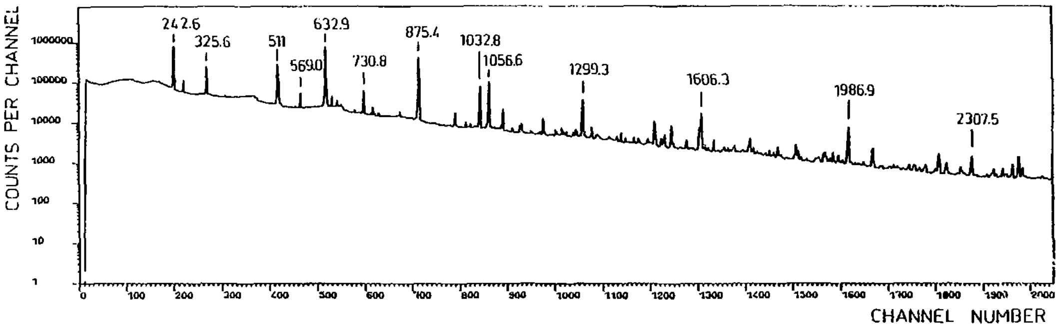

COUNTS PER CHANNEL
CHANNEL NUMBER
242.6
325.6
511
569.0
632.9
730.8
875.4
1032.8
1056.6
1299.3
1606.3
1986.9
2307.5

Fig 1A

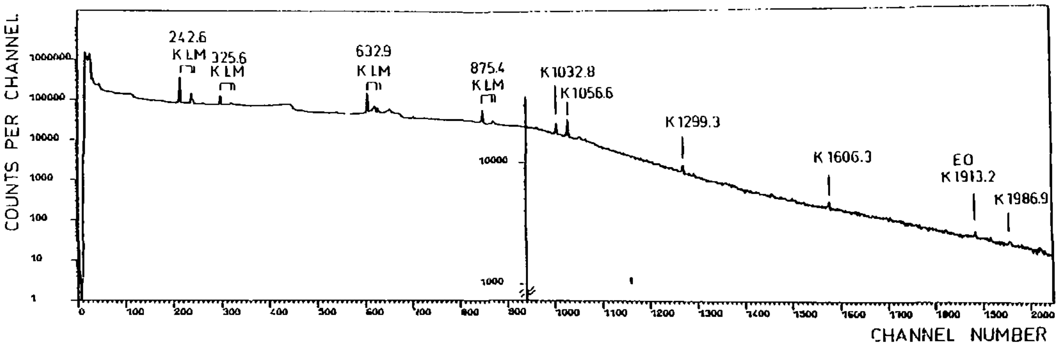
COUNTS PER CHANNEL
CHANNEL NUMBER
242.6
K LM
325.6
K LM
632.9
K LM
875.4
K LM
K 1032.8
K 1056.6
K 1299.3
K 1606.3
EO
K 1913.2
K 1986.9

Fig 1B

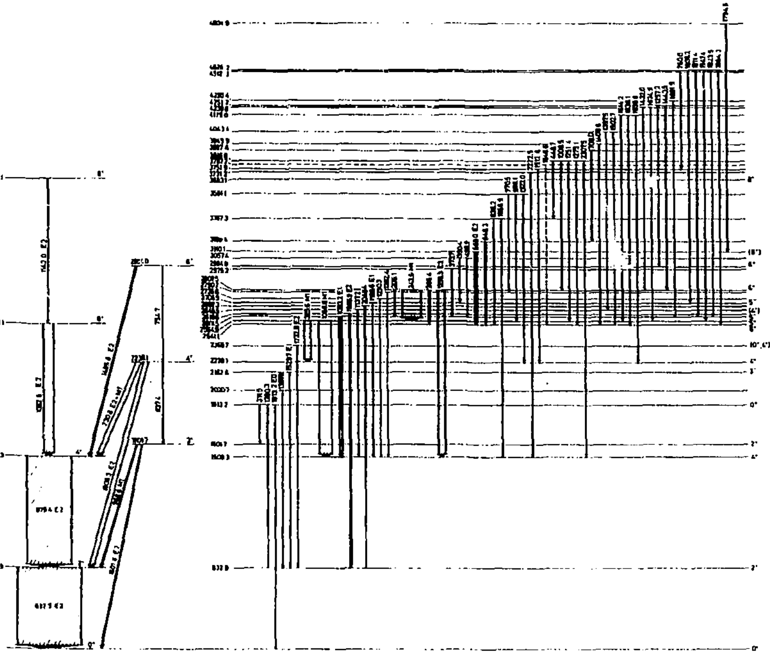

^{108}Cd

Fig 2

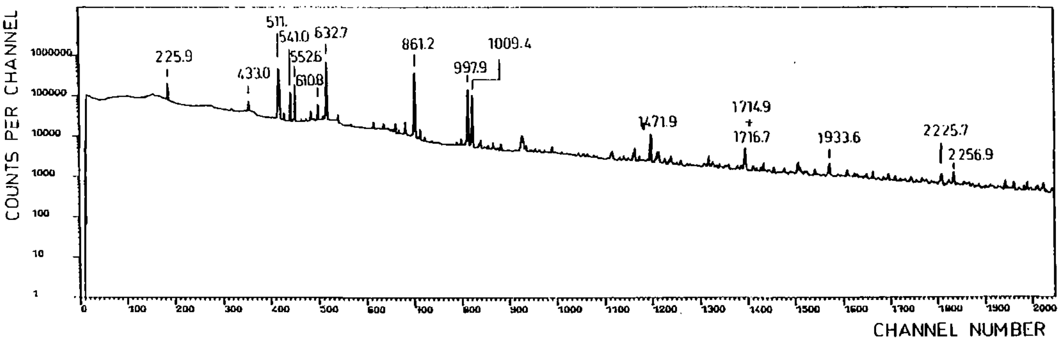
COUNTS PER CHANNEL
1000000
100000
10000
1000
100
10
1
225.9
433.0
511.
541.0
552.6
610.8
632.7
861.2
997.9
1009.4
1471.9
1714.9
+
1716.7
1933.6
2225.7
2256.9
0
100
200
300
400
500
600
700
800
900
1000
1100
1200
1300
1400
1500
1600
1700
1800
1900
2000
CHANNEL NUMBER

Fig 3A

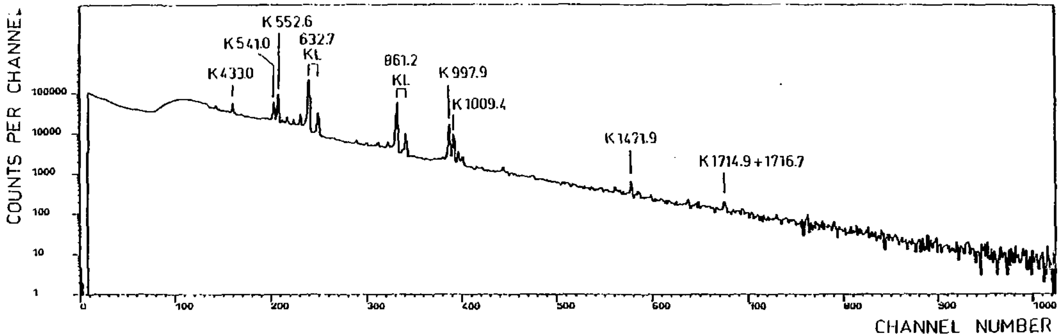

COUNTS PER CHANNEL
100000
10000
1000
100
10
1
K 552.6
K 541.0
632.7
KL
K 433.0
861.2
KL
K 997.9
K 1009.4
K 1421.9
K 1714.9 + 1716.7
0
100
200
300
400
500
600
700
800
900
1000
CHANNEL NUMBER

Fig 3B

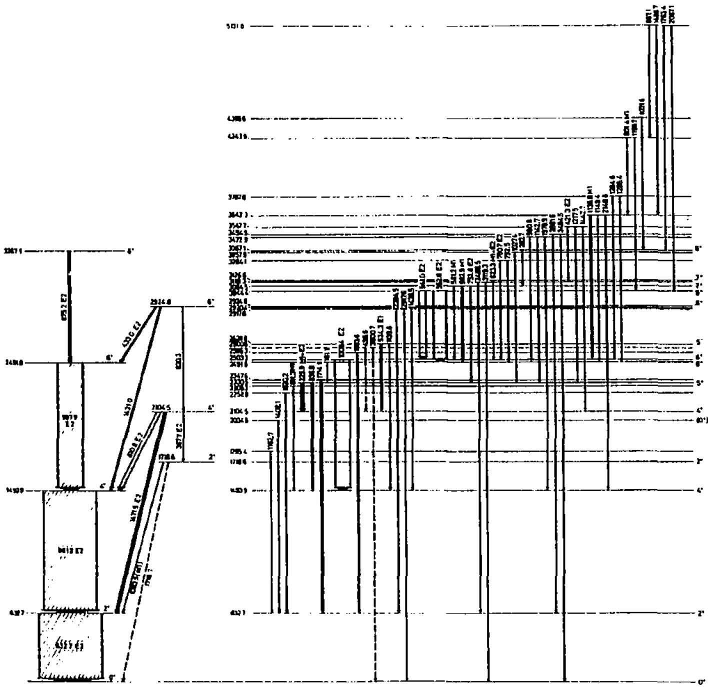

^{106}Cd

Fig 4

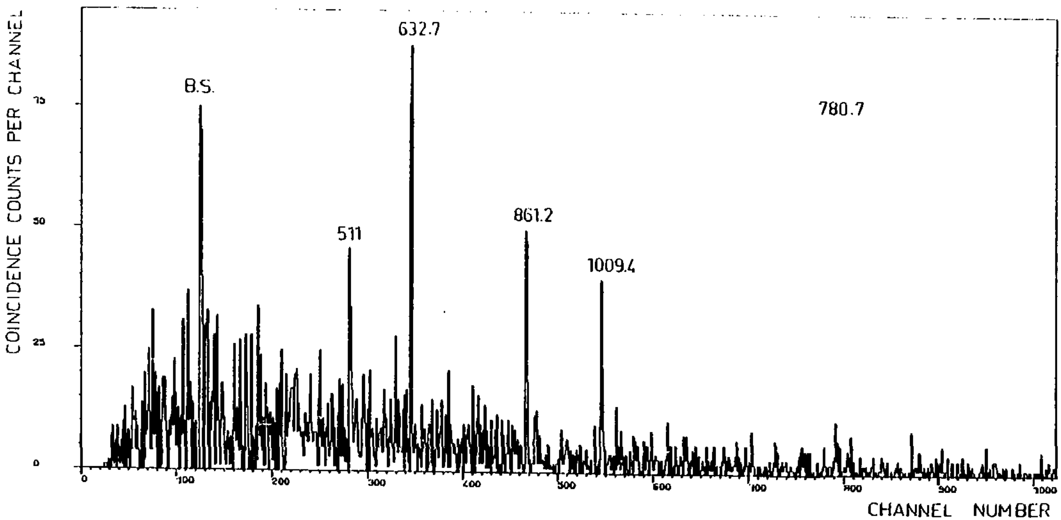
COINCIDENCE COUNTS PER CHANNEL
0
25
50
75
B.S.
632.7
511
861.2
1009.4
780.7
0
100
200
300
400
500
600
700
800
900
1000
CHANNEL NUMBER

Fig 5

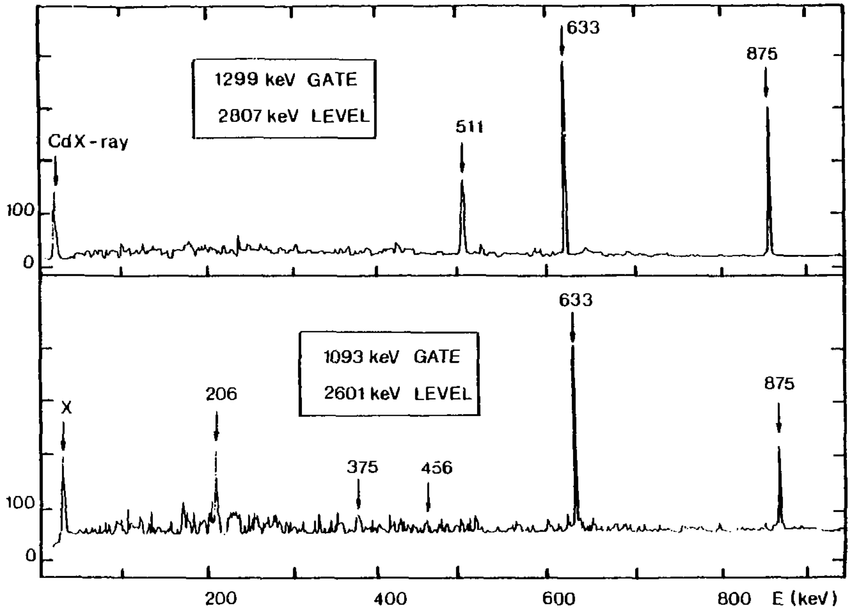
1299 keV GATE
2807 keV LEVEL
CdX-ray
511
633
875
100
0
1093 keV GATE
2601 keV LEVEL
X
206
375
456
633
875
100
0
200
400
600
800
E (keV)

Fig 6

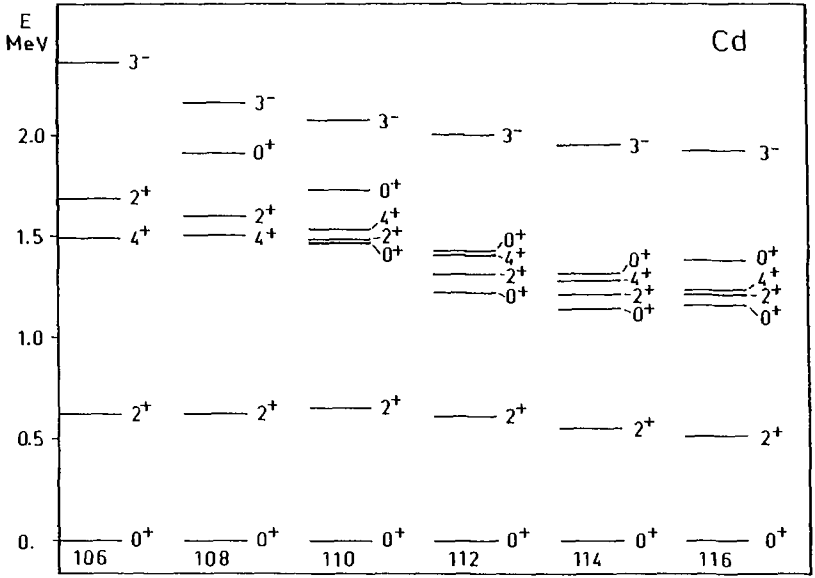

Fig 7

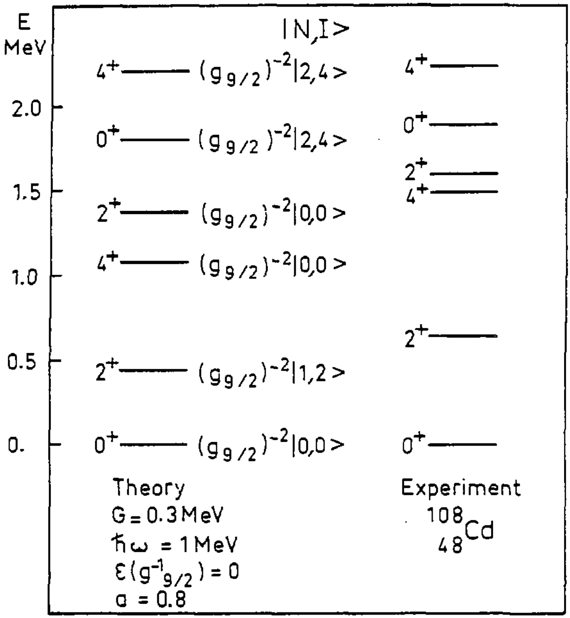
E
MeV
2.0
1.5
1.0
0.5
0.
|N,I>
4+ (g9/2)-2|2,4>
0+ (g9/2)-2|2,4>
2+ (g9/2)-2|0,0>
4+ (g9/2)-2|0,0>
2+ (g9/2)-2|1,2>
0+ (g9/2)-2|0,0>
4+
0+
2+
4+
2+
0+
Theory
G = 0.3 MeV
ħω = 1 MeV
ε(g-1 9/2) = 0
a = 0.8
Experiment
108 48 Cd

Fig 8